Supporting Information

Computational Study of the Reaction of 1-methyl-4-amino-1,2,4-triazolium Dicyanamide with NO_2: From Reaction Dynamics to Potential Surfaces, Kinetics and Spectroscopy

Jianbo Liu* and Wenjing Zhou

Department of Chemistry and Biochemistry, Queens College and the Graduate Center of the City University of New York, 65-30 Kissena Blvd., Queens, New York 11367, USA

Steven D. Chambreau

[†]ERC, Inc., Air Force Research Laboratory, California 93524, USA

Ghanshyam L. Vaghjiani

In-Space Propellants Branch, Rocket Propulsion Division, Aerospace Systems Directorate, Air Force Research Laboratory, AFRL/RQRS, Edwards Air Force Base, California 93524, USA

Table of Contents

Computatioanl methodologies S2

Fig. S1 Comparion of harmonic IR and Raman spectra of MAT^+DCA^- with experiment S7

Tabel S1 Comparion of calcualted harmonic frequencies of MAT^+DCA^- with experiment S8

Fig. S2 Comparion of anharmonic IR and Raman spectra of MAT^+DCA^- with experiment S9

Fig. S3 Harmonic IR and Raman spectra of $HNC(\text{-}NO_2)NCN$, $HNCNC(\text{-}NO_2)N$, $NCNC(\text{-}NO_2)N^-$ and $ON(CN)_2^-$ S10

Cartesian coordinates for the structures in Fig. 1 and Table 2 ..... S11

Cartesian coordinates for the structures in Fig. 3 ..... S13

Cartesian coordinates for the structures in Fig. 5 ..... S17

Cartesian coordinates for the structures in Fig. 7 ..... S18

Computational Methodologies

1. Direct dynamics simulations

The chemical reaction dynamics program, VENUS,[1-2] was used to set up initial conditions for the trajectories. Trajectories started at the equilibrium geometries of reactants. Initial reactant vibrational modes were sampled using the quantum Boltzmann probability distribution:[3]

$$P(n_i) = \exp(-\frac{n_i h\upsilon_i}{k_B T})\,[1 - \exp\left(-\frac{h\upsilon_i}{k_B T}\right)] \qquad (1)$$

where ν_i and n_i are the frequency and the quantum number of the i^{th} vibrational mode, respectively; k_B is the Boltzmann constant, and T is the temperature. Reactant rotational energy (E_{rot}) was sampled from a classical Boltzmann distribution. Vibrational states were simulated by giving individual reactant atoms displacements from equilibrium geometries and momenta that were appropriate to initial rovibrational states, with random phases for different modes. Each molecule had zero point energy (ZPE) in all of its vibrational modes. Collision energy (E_{col}) was added as relative translational energy. Initial separation between the centers of mass of randomly oriented reactants was set in the range of 7 – 9 Å where the inter-molecular interaction was negligible. The purpose of trajectory simulations was to capture gross features and key dynamics of the reaction, therefore, all trajectories were calculated at zero impact parameter (*i.e.* head-on collisions).

The Hessian-based predictor-corrector algorithm,[4] as implemented in Gaussian 09,[5] was used for numerical integration of the classical equations of motion, with the Hessian matrix updated every five steps. Trajectories were propagated with a step size of 0.25 amu$^{1/2}$Bohr which corresponded to a step size of ~ 0.4 fsec in trajectory time and was small enough to ensure that energy conservation was met. Because millions of gradient and Hessian evaluations were required, we had to make a compromise between accuracy and computational cost in selecting the level of theory to be used for the simulations. The B3LYP method has been used successfully in calculating energetics of dialkylimidazolium-[6-10] and triazolium-based[11] ILs, with negligible basis set superposition errors for the ion pairs.[9] In a previous study,[12] we had utilized the B3LYP/6-31G(d) level of theory for reaction dynamics simulations of

$EMIM^+DCA^-$ and $EMMIM^+DCA^-$. The trajectory outcomes in that work were in good agreement with the experiment.[13] By extension, the B3LYP/6-31G(d) level of theory is expected to provide a reliable description of MAT^+DCA^- and was thus chosen for the present work. An initial guess of the molecular orbital for each DFT calculation was obtained from the previous trajectory step, and the total energy of the system was checked at each step to ensure that the energy was conserved to better than 10^{-4} Hartree. A quadratically convergent SCF procedure[5, 14] was adopted for the trajectory integration in those cases when first-order SCF did not converge. It is to be noted that the M06 method was used for the spectral analysis in Kaiser *et al.*'s work.[15] To compare the performance of the B3LYP method vs. the M06 method, we calculated the ion pair energy of MAT^+DCA^- at the B3LYP and the M06 levels of theory with the same 6-31G(d) basis set. The B3LYP-calculated pairing energy (ΔH = 4.27 eV at 298 K) is slightly less than the M06-calculated value (4.44 eV). The two theories produced similar PESs for the $MAT^+DCA^- \rightarrow [MAT^+ - H_{C5}^+]$ + HDCA reaction, with the maximum differences between the two PESs being less than 0.2 eV. A small batch of trajectories for $MAT^+DCA^- + NO_2$ was also carried out at the M06/6-31G(d) level of theory. The M06 trajectories were found to follow similar pathways and revealed similar dynamics as the B3LYP trajectories. Finally, we also computed a few trajectories at the MP2/6-31G(d) level of theory. But the MP2 computational cost was significantly higher than that of B3LYP and M06, presumably due to the fact that the computational requirements for MP2 scales as N^5, whereas DFT scales only as N^{3-4} where N is a measure of the problem size.[16]

Trajectories were terminated after a preset length of time (~ 1 psec) or when product separation exceeded 8.0 Å. All calculations were completed on a Linux computer cluster at Queens College. gOpenMol[17] was used for trajectory visualization. Analyses of individual trajectories and trajectory ensembles were carried out with programs written by us for these purposes, which had automated algorithms to search and sort reaction pathways.

An issue with using quasi-classical direct dynamics methods is that vibrational energy (E_{vib}) is not quantized in the molecules. Lack of quantization may affect how energy is distributed between

vibrational modes.[18-19] It is possible to have trajectories where the product E_{vib} is below ZPE. Such unphysical trajectories were found to be of minor occurrence in our previous reaction dynamics studies of $EMIM^+DCA^-$ and $EMMIM^+DCA^-$ and also in the present study of $MAT^+DCA^- + NO_2$, presumably because here we are looking at high internal energy conditions, for which the errors associated with treating the motion classically are minimalized.

2. Electronic structure calculations and RRKM analysis of reaction PESs

Using trajectory results as a guide, structures of reactants, intermediates, TSs and products along all of the reaction pathways were optimized at the B3LYP/6-311++G(d,p) level of theory. TSs were verified to be first-order saddle points by frequency calculations, and the vibrational mode with an imaginary frequency corresponded to the associated reaction pathway. IRC calculations were carried out to confirm that TSs were located between correct minima. The Cartesian coordinates for all of the reactants, intermediates, TSs and products are provided in the Supporting Information. Reaction PESs were evaluated by the sum of electronic energies, ZPEs and thermal corrections at 298 K, for which the vibrational frequencies and ZPEs were scaled by a factor of 0.955 and 0.981,[20] respectively. To simulate reactant and product IR and Raman spectra in a condensed-phase IL environment, important structures were re-optimized using a parameterized SCRF-based SMD[21] method (also known as the generic ionic liquid solvation model, SMD-GIL)[22] and solvent parameters that were consistent with the experiment.

Statistical outcomes of reaction PESs were predicted using RRKM.[23] The RRKM theory is based on the assumptions of randomized distribution of reaction energy and no TS re-crossing.[24-26] The RRKM reaction rate of a particular process is proportional to the total number of energetically accessible states in the TS. As a consequence, the most probable reactions follow IRC paths for which the density of states is the highest.[27] RRKM densities of states and rate constants were calculated using a direct count algorithm[28] and the scaled frequencies, energetics and moments of inertia of complexes and TSs as determined from the B3LYP/6-311++G(d,p) level of theory calculations. The rotation quantum number K was treated as active, so that all $(2J + 1)$ K-levels were counted in $k(E, J)$ as:[29]

$$k(E,J) = \frac{d}{h}\frac{\sum_{K=-J}^{J} G[E-E_0-E_r^{\dagger}(J,K)]}{\sum_{K=-J}^{J} N[E-E_r(J,K)]} \quad (2)$$

where d is the reaction path degeneracy, G is the sum of accessible states from 0 to $E - E_0 - E_r^{\dagger}$ in the TS, N is the energized reactant′s density of states, E is the system energy, E_0 is the activation energy or the unimolecular dissociation threshold, and E_r and $E_r^{\dagger}$ are the rotational energies for the reactant and the TS, respectively. Orbital angular momentum L was estimated from collision cross section ($\sigma_{collision}$), *i.e.,* $L = \mu \cdot v_{rel} \cdot (\sigma_{collision}/\pi)^{1/2}$, where μ and v_{rel} are the reduced mass and relative velocity, respectively, of the collision partners, and $\sigma_{collision}$ was taken as an orientation-averaged hard-sphere collision cross section.

References

(1) Hase, W. L.; Bolton, K.; de Sainte Claire, P.; Duchovic, R. J.; Hu, X.; Komornicki, A.; Li, G.; Lim, K.; Lu, D.; Peslherbe, G. H.; Song, K.; Swamy, K. N.; Vande Linde, S. R.; Varandas, A.; Wang, H.; Wolf, R. J. *Venus 99: A General Chemical Dynamics Computer Program*, Texas Tech University Lubbock, TX, 1999.

(2) Hu, X.; Hase, W. L.; Pirraglia, T. Vectorization of the General Monte Carlo Classical Trajectory Program Venus. *J. Comput. Chem.* **1991,** *12*, 1014-24.

(3) Peslherbe, G. H.; Wang, H.; Hase, W. L. Monte Carlo Sampling for Classical Trajectory Simulations. *Adv. Chem. Phys.* **1999,** *105*, 171-201.

(4) Bakken, V.; Millam, J. M.; Schlegel, H. B. Ab Initio Classical Trajectories on the Born-Oppenheimer Surface: Updating Methods for Hessian-Based Integrators. *J. Chem. Phys.* **1999,** *111*, 8773-8777.

(5) Frisch, M. J.; Trucks, G. W.; Schlegel, H. B.; Scuseria, G. E.; Robb, M. A.; Cheeseman, J. R.; Scalmani, G.; Barone, V.; Mennucci, B.; Petersson, G. A.; Nakatsuji, H.; Caricato, M.; Li, X.; Hratchian, H. P.; Izmaylov, A. F.; Bloino, J.; Zheng, G.; Sonnenberg, J. L.; Hada, M.; Ehara, M.; Toyota, K.; Fukuda, R.; Hasegawa, J.; Ishida, M.; Nakajima, T.; Honda, Y.; Kitao, O.; Nakai, H.; Vreven, T.; J. A. Montgomery, J.; Peralta, J. E.; Ogliaro, F.; Bearpark, M.; Heyd, J. J.; Brothers, E.; Kudin, K. N.; Staroverov, V. N.; Keith, T.; Kobayashi, R.; Normand, J.; Raghavachari, K.; Rendell, A.; Burant, J. C.; Iyengar, S. S.; Tomasi, J.; Cossi, M.; Rega, N.; Millam, J. M.; Klene, M.; Knox, J. E.; Cross, J. B.; Bakken, V.; Adamo, C.; Jaramillo, J.; Gomperts, R.; Stratmann, R. E.; Yazyev, O.; Austin, A. J.; Cammi, R.; Pomelli, C.; Ochterski, J. W.; Martin, R. L.; Morokuma, K.; Zakrzewski, V. G.; Voth, G. A.; Salvador, P.; Dannenberg, J. J.; Dapprich, S.; Daniels, A. D.; Farkas, O.; Foresman, J. B.; Ortiz, J. V.; Cioslowski, J.; Fox, D. J. Gaussian 09, Rev. B. 01. **2009**.

(6) Kroon, M. C.; Buijs, W.; Peters, C. J.; Witkamp, G.-J. Quantum Chemical Aided Prediction of the Thermal Decomposition Mechanisms and Temperatures of Ionic Liquids. *Thermochimica Acta* **2007,** *465*, 40-47.

(7) Emel'yanenko, V. N.; Verevkin, S. P.; Heintz, A. The Gaseous Enthalpy of Formation of the Ionic Liquid 1-Butyl-3-Methylimidazolium Dicyanamide from Combustion Calorimetry, Vapor Pressure Measurements, and Ab Initio Calculations. *J. Am. Chem. Soc.* **2007,** *129*, 3930-3937.

(8) Verevkin, S. P.; Emel'yanenko, V. N.; Zaitsau, D. H.; Heintz, A.; Muzny, C. D.; Frenkel, M. Thermochemistry of Imidazolium-Based Ionic Liquids: Experiment and First-Principles Calculations. *Phys. Chem. Chem. Phys.* **2010,** *12*, 14994-15000.

(9) Hollóczki, O.; Gerhard, D.; Massone, K.; Szarvas, L.; Németh, B.; Veszprémi, T.; Nyulászi, L. Carbenes in Ionic Liquids. *New J. CHem.* **2010,** *34*, 3004-3009.

(10) Clough, M. T.; Geyer, K.; Hunt, P. A.; Mertes, J.; Welton, T. Thermal Decomposition of Carboxylate Ionic Liquids: Trends and Mechanisms. *Phem. Chem. Chem. Phys.* **2013,** *15*, 20480-20495.

(11) Gao, Y.; Gao, H.; Piekarski, C.; Shreeve, J. n. M. Azolium Salts Functionalized with Cyanomethyl, Vinyl, or Propargylsubstituents and Dicyanamide, Dinitramide, Perchlorate and Nitrate Anions. *Eur. J. Inorg. Chem.* **2007**, 10.1002/ejic.200700666, 4965-4972.

(12) Liu, J.; Chambreau, S. D.; Vaghjiani, G. L. Dynamics Simulations Amd Statistical Modeling of Thermal Decomposition of 1-Ethyl-3-Methylimidazolium Dicyanamide and 1-Ethyl-2,3-Dimethylimidazolium Dicyanamide. *J. Phys. Chem. A* **2014,** *118*, 11133-11144.

(13) Chambreau, S. D.; Schenk, A. C.; Sheppard, A. J.; Yandek, G. R.; Vaghjiani, G. L.; Maciejewski, J.; Koh, C. J.; Golan, A.; Leone, S. R. Thermal Decomposition Mechanims of Alkylimidazolium Ionic Liquids with Cyano-Containing Anions. *J. Phys. Chem. A* **2014,** *118*, 11119-11132.

(14) Bacskay, G. B. A Quadratically Convergent Hartree-Fock (QC-SCF) Method. Application to Closed Shell Systems. *Chem. Phys.* **1981,** *61*, 385-404.

(15) Brotton, S. J.; Lucas, M.; Chambreau, S. D.; Vaghjiani, G. L.; Yu, J.; Anderson, S. L.; Kaiser, R. I. Spectroscopic Investigation of the Primary Reaction Intermediates in the Oxidation of Levitated Droplets of Energetic Ionic Liquids. *J. Phys. Chem. Lett.* **2017,** *8*, 6053-6059.

(16) Sun, R.; Siebert, M. R.; Xu, L.; Chambreau, S. D.; Vaghjiani, G. L.; Lischka, H.; Liu, J.; Hase, W. L. Direct Dynamics Simulation of the Activation and Dissociation of 1,5-Dinitrobiuret (HDNB). *J. Phys. Chem. A* **2014,** *118*, 2228-2236.

(17) Laaksonen, L. *gOpenMol*, 3.0; Center for Scientific Computing: Espoo, Finland, 2005.

(18) Untch, A.; Schinke, R.; Cotting, R.; Huber, J. R. The Vibrational Predissociation of *cis*-Methyl Nitrite in the S_1 State: A Comparison of Exact Quantum Mechanical Wave Package Calculation with Classical Trajectory Calculations and Detailed Experimental Results. *J. Chem. Phys.* **1993,** *99*, 9553-9566.

(19) Miller, W. H.; Hase, W. L.; Darling, C. L. A Simple Model for Correcting the Zero Point Energy Problem in Classical Trajectory Simulations of Polyatomic Molecules. *J. Chem. Phys.* **1989,** *91*, 2863-2868.

(20) Zheng, J.; Alecu, I. M.; Lynch, B. J.; Zhao, Y.; Truhlar, D. G. Database of Frequency Scale Factors for Electronic Model Chemistries, Version 2. http://comp.chem.umn.edu/freqscale/version2.htm: 2010.

(21) Marenich, A. V.; Cramer, C. J.; Truhlar, D. G. Universal Solvation Model Based on Solute Electron Density and on a Continuum Model of the Solvent Defined by the Bulk Dielectric Constant and Atomic Surface Tensions. *J. Phys. Chem. B* **2009,** *113*, 6378-6396.

(22) Bernales, V. S.; Marenich, A. V.; Contreras, R.; Cramer, C. J.; Truhlar, D. G. Quantum Mechanical Continuum Solvation Models for Ionic Liquids. *J. Phys. Chem. B* **2012,** *116*, 9122-9129.

(23) Marcus, R. A. Unimolecular Dissociations and Free-Radical Recombination Reactions. *J. Chem. Phys.* **1952,** *20*, 359-364.

(24) Baer, T.; Hase, W. L. *Unimolecular Reaction Dynamics: Theory and Experiments*. Oxford University Press: New York, 1996, p 438.

(25) Hase, W. L. Some Recent Advances and Remaining Questions Regarding Unimolecular Rate Theory. *Acc. Chem. Res.* **1998,** *31*, 659-665.

(26) Ma, X.; Hase, W. L. Perspective: Chemical Dynamics Simulations of Non-Statistical Reaction Dynamics. *Philos. Trans. R. Soc., A* **2017,** *375*, 20160204.

(27) Fukui, K. A Formulation of the Reaction Coordinate. *J. Phys. Chem.* **1970,** *74*, 461-463.

(28) Zhu, L.; Hase, W. L. *A General RRKM Program (QCPE 644), Quantum Chemistry Program Exchange*, Chemistry Department, University of Indiana: Bloomington, 1993.

(29) Zhu, L.; Hase, W. L. Comparison of Modes for Calculating the RRKM Unimolecular Constant k(E,J). *Chem. Phys. Lett.* **1990,** *175*, 117-124.

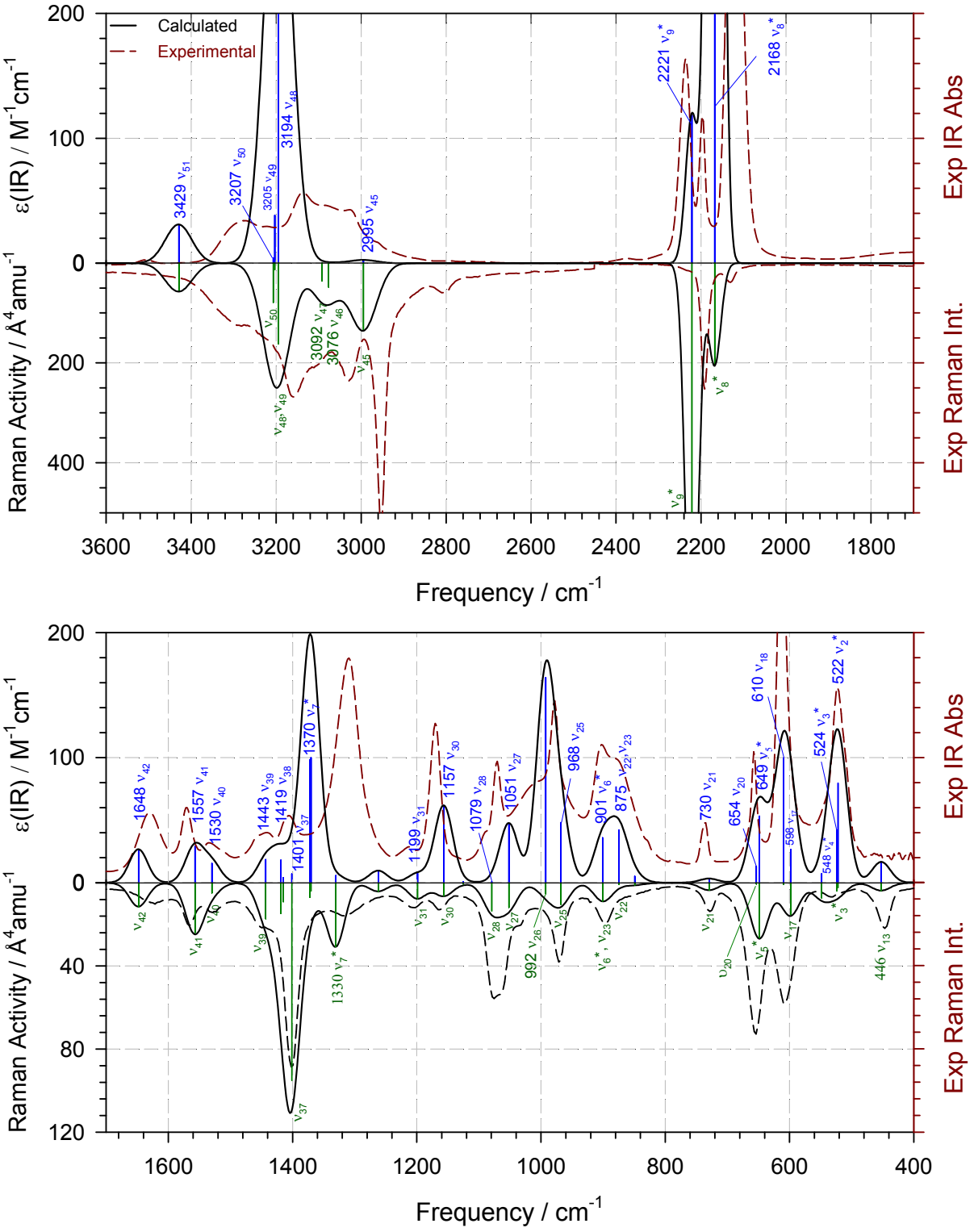

Fig. S1 Comparison of the SMD-GIL//B3LYP/6-311++G(d,p)-calculated harmonic IR and Raman spectra of $MAT^{+}DCA^{-}$ with the experimental spectra available in Ref [9]. The calculated frequencies were scaled by a factor of 0.974. See Table S1 for the assignments of vibrations.

Table S1 Comparison of the SMD-GIL//B3LYP/6-311++G(d,p)-calculated harmonic frequencies of MAT^+DCA^- with the experimental values

	Vibrational mode	Calculated frequencies (cm^{-1})	Experimental IR (cm^{-1}) [a]	Experimental Raman (cm^{-1}) [a]
ν_{13}	antisymmetric NH_2, CH_3 in-plane wag	446		446
ν_2*	in-plane antisymmetric N-C≡N bend of DCA^-	522	511	
ν_3*	out-of-plane antisymmetric N-C≡N bend of DCA^-	524	524	532
ν_4*	out-of-plane symmetric N-C≡N bend of DCA^-	548	540	
ν_{17}	symmetric N-NH_2 and N-CH_3 stretch	598	601	606
ν_{18}	N(4) umbrella	610	613	
ν_{20}, ν_5*	H_3CN(1)-N(2)CH torsion in-plane C-N-C bend of DCA^-	654 649	657	655
ν_{21}	antisymmetric ring mode with N-CH_3 and N-NH_2 stretch	730	737	729
ν_{22} ν_{23}	C(3)H, C(5)H antisymmetric out-of-plane wag C(3)H, C(5)H symmetric out-of-plane wag	875	880	863
ν_6*	C-N-C symmetric stretch of DCA^-	901	905	897
ν_{25}	NH_2 rock	968	978	971
ν_{26}	N(1)-N(2) stretch, C(3)H in-plane wag	992		1038
ν_{27}	ring C-N-C symmetric stretch, C(5) wag and CH_3 rock	1051	1071	1059
ν_{28}	N-C-N ring bend, CH_3 rock	1079	1091	1077
ν_{30}	C(5)H wag, N(1)-CH_3 stretch	1157	1171	1163
ν_{31}	C(3)H, C(5)H antisymmetric in-plane wag	1199	1212	1206
ν_7*	C-N-C antisymmetric stretch of DCA^-	1370	1310	1315
ν_{37}	CH_2 wag	1401	1407	1402
ν_{38}	CH_2 wag 2	1419	1439	
ν_{39}	N(2)-C(3) and N(4)-C(5) symmetric stretch	1443	1455	1448
ν_{40}	N(2)-C(3) and N(4)-C(5) antisymmetric stretch	1530	1535	1530
ν_{41}	N(1)-C(5) stretch, N-NH_2 and N-CH_3 antisymmetric stretch	1557	1571	1566
ν_{42}	NH_2 scissor	1648	1630	1624
ν_8*	C≡N antisymmetric stretch of DCA^-	2168	2126	2132
ν_9*	C≡N symmetric stretch of DCA^-	2221	2197	2191
ν_{45}	CH_3 symmetric stretch	2995	2971	2954
ν_{46}	CH_3 antisymmetric stretch	3076	3022	3029
ν_{47}	CH_3 antisymmetric stretch 2	3092	3080	3109
ν_{48}	C(5)H stretch	3194	3142	3160
ν_{49}	C(3)H stretch	3205	3227	3160
ν_{50}	symmetric NH stretch	3207	3294	3319
ν_{51}	antisymmetric NH stretch	3429	3507	

[a] Ref [9] in the main text.

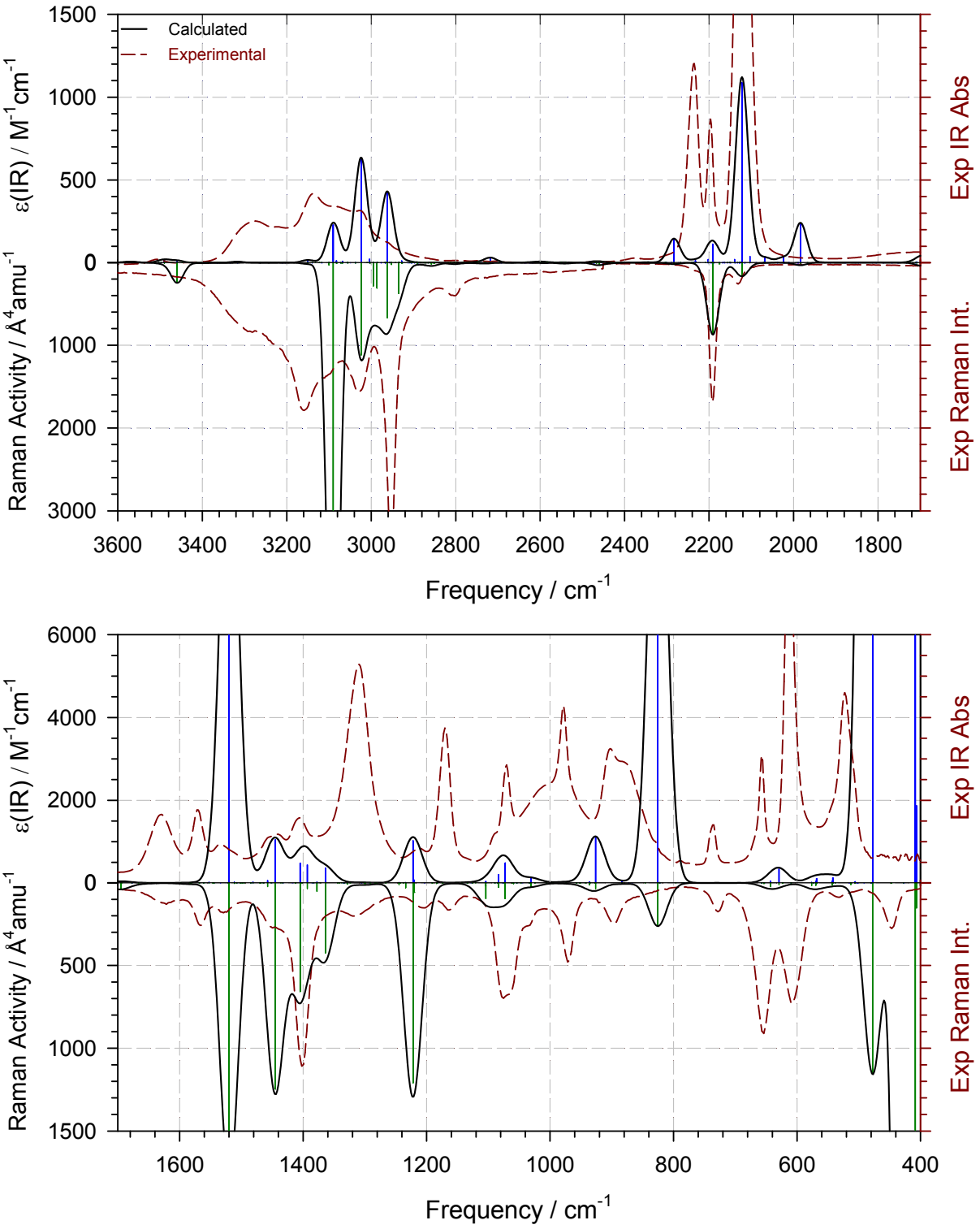

Fig. S2 Comparison of the SMD-GIL//B3LYP/6-311++G(d,p)-calculated anharmonic IR and Raman spectra of $MAT^{+}DCA^{-}$ with experimental data (Ref [9]). The calculated frequencies were scaled by a factor of 0.977.

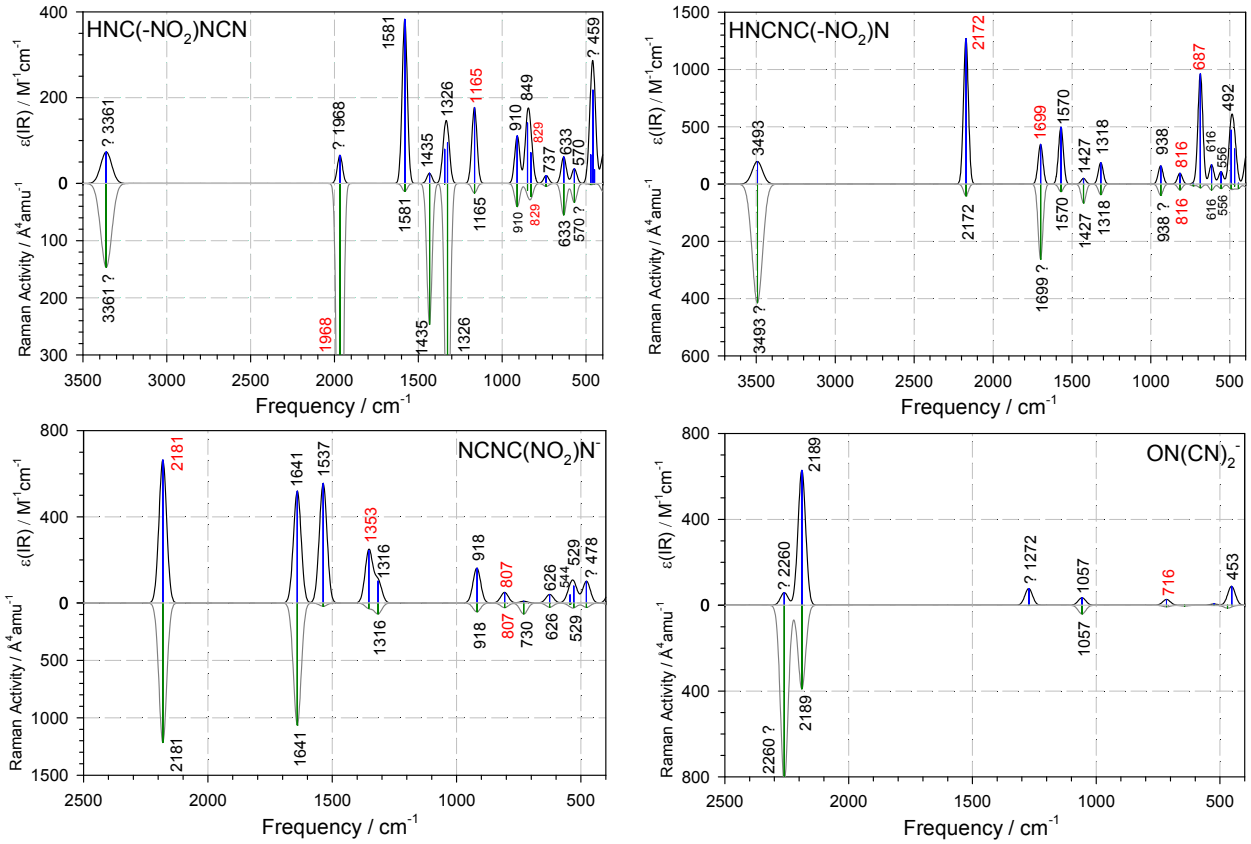

Fig. S3 Harmonic IR (top) and Raman (bottom) spectra of HNC(-NO_2)NCN, HNCNC(-NO_2)N, NCNC(-NO_2)N^- and ON$(CN)_2^-$ simulated at the SMD-GIL//B3LYP/6-311++G(d,p) levels of theory. Frequencies were scaled by a factor of 0.974. Red-labled peaks are product-like, black-labeled ones are close to reactant vibrations, and the peaks that do not match experiemntal results are indciated by question marks.

Cartesian coordinates for the structures in Fig. 1 and Table 2, calculated at B3LYP/6-311++G(d,p)

MAT^+DCA^-

C1 -0.691749 0.107028 0.509083
N2 -1.222356 -1.117349 0.313312
N3 -1.527076 0.971430 -0.043913
C4 -1.392241 2.431023 -0.102347
H5 -2.126930 2.882169 0.564436
H6 -1.579458 2.742921 -1.128277
C7 -2.385138 -0.926420 -0.383213
H8 -3.016158 -1.741951 -0.694762
H9 0.240553 0.363141 0.991535
H10 -0.372663 2.684244 0.194530
N11 3.074503 0.185858 -0.382078
C12 2.411123 1.195084 0.115733
C13 2.437017 -0.948416 -0.426236
N14 1.807958 2.095855 0.561693
N15 1.875000 -1.976330 -0.471829
N16 -2.598139 0.341190 -0.607143
N17 -0.702387 -2.384287 0.624770
H18 0.246171 -2.442094 0.195300
H19 -0.618104 -2.452796 1.635435

TS(PT1)

C1 1.215713 -0.139436 0.094380
N2 1.506459 1.188375 0.009600
N3 2.420262 -0.706198 0.014147
C4 2.716234 -2.134205 0.053227
H5 3.370864 -2.345573 0.898611
H6 3.209398 -2.428149 -0.873247
C7 2.864654 1.345992 -0.114761
H8 3.345387 2.306592 -0.198279
H9 -0.087154 -0.746939 0.217744
H10 1.776531 -2.671071 0.164219
N11 -3.433809 -0.761336 -0.531636
C12 -2.285725 -0.953905 -0.051921
C13 -4.336505 0.082286 -0.066709
N14 -1.200732 -1.241103 0.330433
N15 -5.178889 0.810157 0.267514
N16 3.458076 0.190083 -0.115905
N17 0.612740 2.271424 0.043877
H18 -0.036706 2.186475 -0.732859
H19 0.086712 2.234462 0.912301

$[MAT^+ - H_{C5}^+]\cdot HDCA$

C1 -1.267812 -0.087128 -0.156222
N2 -1.743487 1.191661 -0.058643
N3 -2.379329 -0.799315 0.072486
C4 -2.491386 -2.251624 0.095930
H5 -3.218628 -2.574034 -0.649650
H6 -2.816199 -2.579457 1.083946
C7 -3.088535 1.173527 0.216551
H8 -3.683893 2.063400 0.336946
H9 0.369160 -0.642396 -0.511751
H10 -1.514024 -2.670431 -0.132782
N11 3.538817 -0.795446 0.346499
C12 2.422197 -0.811003 -0.206193
C13 4.490370 0.114882 0.234804
N14 1.371087 -0.980083 -0.738676
N15 5.371860 0.868982 0.201758
N16 -3.515127 -0.049318 0.305829
N17 -1.022230 2.387480 -0.213583
H18 -0.287111 2.416612 0.486973
H19 -0.589430 2.386665 -1.132593

$[MAT^+ - H_{C5}^+]$

C1 0.015014 -1.000571 0.000013
N2 1.065040 -0.116546 0.000016
N3 -1.017538 -0.137805 -0.000014
C4 -2.427131 -0.491209 -0.000026
H5 -2.913334 -0.086433 -0.889292
H6 -2.913335 -0.086509 0.889274
C7 0.615903 1.181366 -0.000007
H8 1.265779 2.040865 -0.000011
H9 -2.494976 -1.576533 -0.000071
N10 -0.681469 1.208355 -0.000025
N11 2.434751 -0.439357 0.000037
H12 2.613828 -1.015683 0.817842
H13 2.613835 -1.015751 -0.817718

HDCA

H1 2.845933 -0.520152 0.613874
N2 -0.063423 0.580084 0.017050
C3 1.059336 0.083233 0.020988
C4 -1.271048 0.041734 0.003509
N5 2.201703 -0.269510 -0.122870
N6 -2.363375 -0.343381 -0.002874

$HN(CN)_2$

N1 0.000088 0.679993 0.000531
C2 1.182270 0.037906 -0.000489
C3 -1.182354 0.038008 0.000105
N4 2.207784 -0.493440 0.000138
N5 -2.207831 -0.493426 -0.000135
H6 0.000215 1.692623 -0.001436

[$MAT^+ – H_{amino}^+$]

C1	-0.059703	-0.910227	-0.020328
N2	-1.179520	-0.146319	0.006046
N3	1.010356	-0.068306	-0.046980
C4	2.415980	-0.418138	0.033562
H5	2.697805	-0.681725	1.056876
H6	2.988450	0.449331	-0.288224
C7	-0.701810	1.157876	0.010681
H8	-1.367410	2.002554	0.021224
H9	-0.028352	-1.983977	-0.041769
H10	2.625523	-1.258511	-0.630463
N11	0.610223	1.209927	-0.014300
N12	-2.482917	-0.431675	0.016412
H13	-2.549809	-1.450133	0.010620

MAT^+

C1	-0.007623	-0.893509	0.000000
N2	-1.094827	-0.091110	0.000000
N3	1.045887	-0.096681	0.000001
C4	2.470775	-0.454696	-0.000001
H5	2.933048	-0.035625	0.892404
H6	2.933042	-0.035651	-0.892421
C7	-0.624667	1.199402	0.000000
H8	-1.273987	2.060896	0.000000
H9	-0.010775	-1.972071	0.000001
H10	2.558277	-1.539358	0.000015
N11	0.678001	1.215645	0.000000
N12	-2.453433	-0.417180	0.000000
H13	-2.699951	-0.930038	-0.840781
H14	-2.699950	-0.930039	0.840780

DCA^-

N1	-0.000014	0.679121	-0.000008
C2	-1.149914	0.058004	0.000028
C3	1.149938	0.058069	-0.000005
N4	-2.233964	-0.389293	-0.000013
N5	2.233958	-0.389319	0.000002

Cartesian coordinates for the structures in Fig. 3, calculated at B3LYP/6-311++G(d,p)

HDCA
H1 2.845933 -0.520152 0.613874
N2 -0.063423 0.580084 0.017050
C3 1.059336 0.083233 0.020988
C4 -1.271048 0.041734 0.003509
N5 2.201703 -0.269510 -0.122870
N6 -2.363375 -0.343381 -0.002874

NO_2
N1 0.000000 0.000000 0.321839
O2 0.000000 1.099987 -0.140804
O3 0.000000 -1.099987 -0.140804

TS1
N1 -3.815819 0.282084 0.009667
C2 -2.667584 0.108427 -0.014542
N3 -1.360154 0.034011 -0.051689
C4 -0.507413 -0.871868 0.007547
N5 0.768309 -0.993606 0.065248
N6 1.883260 0.247477 0.004127
O7 3.007106 -0.162152 -0.050506
O8 1.423291 1.343896 0.034985
H9 1.277622 -1.863064 -0.025322

HN(-NO_2)CNCN
N1 3.730018 0.291528 -0.000016
C2 2.586233 0.089322 -0.000008
N3 1.280041 -0.013854 0.000000
C4 0.456543 -0.951868 0.000024
N5 -0.866488 -0.952552 0.000025
N6 -1.769735 0.239120 -0.000003
O7 -2.940538 -0.060974 0.000010
O8 -1.242119 1.314722 -0.000035
H9 -1.412248 -1.804409 0.000051

TS2
N1 1.084120 1.862411 -0.242899
C2 0.270490 0.988282 0.054405
N3 -0.957190 0.870407 0.497873
C4 -1.898391 0.134202 0.028180
N5 -2.845415 -0.472059 -0.324236
H6 2.035581 1.526673 -0.393216
N7 1.004318 -0.735440 0.033262
O8 0.259945 -1.674205 0.052011
O9 2.206430 -0.693146 -0.033298

HNC(-NO_2)NCN
N1 -1.287607 1.732564 0.000128
C2 -0.419510 0.804923 0.000052
N3 0.902933 1.040191 0.000008
C4 1.874328 0.204665 -0.000065
N5 2.894145 -0.392670 -0.000129
H6 -2.230927 1.331303 0.000152
N7 -0.920898 -0.692929 0.000006
O8 -0.074675 -1.560170 -0.000083
O9 -2.127574 -0.839696 0.000063

TS4
N1 1.281194 1.848383 -0.192939
C2 0.409266 1.031334 0.032810
N3 -0.892891 0.982703 0.356635
C4 -1.777362 0.185017 0.042589
N5 -2.779834 -0.390516 -0.289889
N6 1.105507 -0.667374 0.021051
O7 0.249022 -1.517269 0.110997
O8 2.288472 -0.785623 -0.082726
H9 -3.089215 -1.287346 0.057430

HNCNC(-NO_2)N
N1 -1.331179 1.764927 0.145334
C2 -0.485365 0.861819 -0.034814
N3 0.840900 0.983456 -0.293325
C4 1.773530 0.220465 -0.035897
N5 2.804330 -0.317856 0.269349
N6 -1.053960 -0.622151 -0.017747
O7 -0.221039 -1.503914 -0.113117
O8 -2.248262 -0.748031 0.096101
H9 3.204774 -1.136770 -0.164881

TS5
N1 3.747196 0.325316 -0.383125
C2 2.655169 -0.023755 0.002752
N3 1.568348 -0.242841 0.524666
C4 0.292991 -0.147686 0.255129
N5 -0.716947 -0.831870 0.109641
H6 4.433673 -0.291287 -0.799967
N7 -2.067987 0.101357 -0.071878
O8 -3.029558 -0.552883 -0.341455
O9 -1.950055 1.284908 0.091149

HNCNCN-NO_2
N1 3.751730 -0.175167 -0.438794
C2 2.638571 0.007563 -0.013942
N3 1.542620 0.362207 0.403784
C4 0.274365 0.201418 0.035935
N5 -0.746329 -0.025716 0.718213

H6 4.410943 -0.876180 -0.131209
N7 -2.010405 -0.056719 -0.047334
O8 -2.502449 -1.151776 -0.167496
O9 -2.454036 1.013033 -0.388983

TS_HT
N1 -4.282713 0.775677 0.339393
C2 -3.338126 0.179522 -0.005456
N3 -2.358993 -0.555431 -0.452752
C4 -1.121266 -0.412965 -0.189252
N5 0.039716 -0.371713 -0.052517
N6 2.889377 0.318865 -0.208376
O7 4.045607 0.563950 -0.232616
O8 2.390298 -0.475925 0.658783
H9 1.257406 -0.475333 0.378663

DCA
N1 0.000023 0.656080 0.000097
C2 -1.147556 0.054284 -0.000075
C3 1.147552 0.054307 -0.000197
N4 -2.240223 -0.374569 0.000041
N5 2.240204 -0.374589 0.000095

HNO_2 (*trans*-conformation)
N1 0.180051 0.486565 0.000068
O2 -1.045306 -0.255258 0.000055
O3 1.102795 -0.225557 -0.000053
H4 -1.720273 0.440558 -0.000488

TS_HT′
N1 -3.836117 0.740424 -0.535995
C2 -2.919528 0.218737 -0.033648
N3 -1.961450 -0.360173 0.636504
C4 -0.841823 -0.751011 0.187276
N5 0.201764 -1.219823 -0.121542
N6 2.332418 0.206495 -0.044694
O7 3.371146 -0.333866 -0.351896
O8 2.132807 1.348706 0.306642
H9 1.380178 -0.493541 -0.099652

O-NH-O
N1 0.000000 0.000000 0.309894
O2 0.000000 1.094283 -0.220195
O3 0.000000 -1.094283 -0.220195
H4 0.000000 0.000000 1.353866

TS1′
N1 -4.041721 0.352616 0.319180
C2 -2.958950 0.002810 0.092310
N3 -1.781558 -0.523890 -0.182319
C4 -0.621709 -0.065241 -0.190912
N5 0.589730 -0.405767 -0.380221
N6 2.830884 0.532975 0.155069
O7 3.068322 -0.613574 0.359148
O8 1.582097 0.848468 -0.208973
H9 1.099268 -1.196108 0.008247

HN(-ONO)CNCN
N1 -3.800840 0.552715 -0.248800
C2 -2.728781 0.164307 -0.026333
N3 -1.561608 -0.311590 0.337816
C4 -0.425766 -0.353602 -0.202767
N5 0.695115 -0.814960 0.342937
N6 2.694174 0.482466 -0.316143
O7 2.165850 1.283091 0.294841
O8 1.833094 -0.913429 -0.385720
H9 0.747848 -1.181934 1.290963

TS2′
N1 -2.713108 -0.333855 -0.430433
C2 -1.738886 0.119109 0.028454
N3 -0.707805 0.624953 0.647964
C4 0.396193 1.036337 0.083349
N5 1.217813 1.947701 -0.005714
N6 1.162648 -1.423968 -0.292435
O7 0.724507 -1.635415 0.794035
O8 1.079313 -0.297964 -0.857210
H9 0.908756 2.830539 0.398904

HNC(-ONO)NCN
N1 2.957232 -0.992372 -0.186702
C2 2.123075 -0.163030 -0.142009
N3 1.303302 0.837348 -0.145212
C4 -0.023244 0.667887 0.202568
N5 -0.869537 1.644752 0.086015
N6 -1.900966 -1.122516 0.156268
O7 -2.435486 -0.484193 -0.596631
O8 -0.395332 -0.523822 0.664417
H9 -0.382659 2.464498 -0.278219

TS3′
N1 1.001911 2.351777 0.054758
C2 1.216933 1.164851 -0.143898
N3 0.660758 -0.008221 -0.025248
C4 1.305034 -1.178233 -0.040118
N5 1.822231 -2.212612 -0.066093
H6 1.600739 3.100268 -0.272656
N7 -1.751680 -0.127483 -0.462768
O8 -2.824808 -0.219044 -0.031793
O9 -0.783328 -0.161481 0.640819

HNCN(-ONO)CN
N1 0.190850 2.398052 -0.048075
C2 0.925113 1.408147 -0.130587
N3 0.638977 0.102327 0.136075
C4 1.538512 -0.881089 -0.031270
N5 2.290281 -1.749251 -0.167211
H6 0.545161 3.325105 -0.256467
N7 -1.623893 -0.501961 -0.490351
O8 -2.641486 -0.751819 -0.046085
O9 -0.583567 -0.277132 0.697903

TS4′
N1 -2.457678 -1.422935 0.177758
C2 -1.885417 -0.408041 -0.096637
N3 -1.481932 0.737312 -0.320617
C4 -0.322017 1.298593 -0.016901
N5 0.418976 2.221067 0.114621
H6 -2.445231 -2.305740 -0.311674
N7 1.953178 -0.275023 -0.293143
O8 2.497839 -1.310013 -0.089550
O9 0.834914 -0.172552 0.494871

HNCNC(-ONO)N
N1 3.494167 -0.106598 0.264020
C2 2.317675 -0.291235 0.056257
N3 1.130175 -0.596884 0.003806
C4 0.034147 0.251702 -0.184218
N5 0.075653 1.513314 -0.107118
H6 4.205771 -0.080409 -0.453103
N7 -2.301123 0.106224 0.447207
O8 -3.282025 -0.335058 0.081846
O9 -1.106576 -0.426791 -0.461162

TS5′
N1 -3.949870 -0.094592 -0.441202
C2 -2.829047 -0.029239 0.008556
N3 -1.717300 -0.194700 0.497183
C4 -0.474116 0.159147 0.257753
N5 0.632197 -0.356738 0.134091
H6 -4.631688 0.652404 -0.405266
N7 2.966304 0.387194 -0.154489
O8 3.167246 -0.773505 -0.183633
O9 1.699172 0.821005 0.003424

HNCNCN-ONO
N1 -4.007544 0.041825 -0.088221
C2 -2.814030 -0.120879 0.019430
N3 -1.624660 -0.402818 -0.033472
C4 -0.488286 0.319395 -0.017772
N5 0.682026 -0.129325 -0.004924
H6 -4.661258 0.098770 0.679980
N7 3.036169 0.292114 0.011450
O8 3.077744 -0.862318 0.015624
O9 1.656408 0.874513 -0.001094

NO
N1 0.000000 0.000000 -0.612285
O2 0.000000 0.000000 0.535749

HN(O)CNCN
N1 -2.975840 -0.217671 -0.250202
C2 -1.867271 -0.046804 0.034676
N3 -0.637587 0.163419 0.516955
C4 0.400252 0.256486 -0.153248
N5 1.694948 0.370890 -0.102239
O6 2.520688 -0.595807 -0.007089
H7 2.065971 1.291893 -0.383448

HNC(O)NCN
N1 2.436805 -0.398988 -0.257299
C2 1.379209 -0.087186 0.092104
N3 0.187601 0.269191 0.608624
C4 -1.035364 -0.110371 0.008899
N5 -0.706460 1.171918 -0.364622
O6 -1.797241 -1.001000 -0.092843
H7 -1.110768 1.898495 0.229800

HNCN(O)CN
N1 2.139446 -0.718468 -0.166566
C2 1.065790 -0.244746 0.124026
N3 -0.053048 0.386381 -0.007145
C4 -1.209531 -0.362236 0.006869
N5 -2.208460 -0.939518 -0.010985
H6 2.770543 -1.044902 0.567014
O7 -0.131708 1.698504 -0.007440

HNCNC(O)N
N1 -2.549614 0.195423 -0.134112
C2 -1.415796 -0.163300 0.025052
N3 -0.293446 -0.675542 0.046514
C4 0.898009 -0.019347 0.009650
N5 1.367707 1.158114 0.005877
H6 -3.216186 0.504698 0.557003
O7 2.081298 -0.519348 -0.024145

HNCNCNO
N1 2.921205 -0.287812 -0.127105
C2 1.769061 0.051479 0.023620
N3 0.644690 0.542457 0.016331
C4 -0.573267 0.016118 -0.000330

N5 -1.738517 -0.016964 0.001950
H6 3.545601 -0.515370 0.636186
O7 -2.939002 -0.194248 -0.001770

HNCO
C1 -0.044851 0.021878 -0.000210
N2 1.158127 -0.122263 0.000066
O3 -1.210324 0.013896 0.000085
H4 1.844813 0.613402 0.000122

NCN
C1 0.000000 0.089813 0.000000
N2 1.211058 -0.039982 0.000000
N3 -1.211058 -0.037001 0.000000

HNCN
N1 1.155561 -0.133976 0.000003
C2 -0.109034 0.009343 -0.000010
N3 -1.299271 0.018057 0.000004
H4 1.660174 0.755376 0.000004

NCO
C1 0.000000 0.047048 0.000000
N2 0.624492 1.082804 0.000000
O3 -0.546431 -0.982739 0.000000

Cartesian coordinates for the structures in Fig. 5, calculated at B3LYP/6-311++G(d,p)

DCA^-
N1 -0.000014 0.679121 -0.000008
C2 -1.149914 0.058004 0.000028
C3 1.149938 0.058069 -0.000005
N4 -2.233964 -0.389293 -0.000013
N5 2.233958 -0.389319 0.000002

NO_2
N1 0.000000 0.000000 0.321839
O2 0.000000 1.099987 -0.140804
O3 0.000000 -1.099987 -0.140804

TS6
N1 -1.283945 0.202315 0.000008
C2 -0.428996 -0.766888 0.000004
C3 -2.589175 0.094402 -0.000005
N4 0.796286 -1.071810 0.000007
N5 -3.757869 0.125066 -0.000016
N6 1.812440 0.123243 0.000003
O7 2.980330 -0.225413 0.000019
O8 1.412250 1.273315 -0.000021

$NCNCN\text{-}NO_2^-$
N1 -1.252353 0.186243 0.000615
C2 -0.410298 -0.793880 -0.000862
C3 -2.559657 0.083572 0.000362
N4 0.854655 -1.020821 -0.001011
N5 -3.727546 0.120608 0.000333
N6 1.762400 0.107739 -0.000038
O7 2.952445 -0.196582 0.001480
O8 1.342510 1.259766 -0.001016

TS7
N1 -1.084031 0.876016 0.426036
C2 0.183605 1.027361 0.105712
C3 -1.878426 -0.029414 -0.099371
N4 1.013765 1.940807 -0.053028
N5 -2.696118 -0.775883 -0.502541
N6 1.095613 -0.541408 0.036737
O7 1.992687 -0.686234 -0.783151
O8 0.740354 -1.374316 0.859592

$NCNC(\text{-}NO_2)N^-$
N1 -0.948207 1.092610 -0.000028
C2 0.365571 0.946558 0.000121
C3 -1.804238 0.104121 -0.000186
N4 1.345979 1.748416 0.000307
N5 -2.657795 -0.696988 -0.000331
N6 0.931640 -0.564298 0.000051
O7 1.120718 -1.085068 -1.085676
O8 1.120618 -1.085213 1.085726

TS7′
N1 1.540787 0.586837 0.378700
C2 0.421308 1.129891 0.022193
C3 1.972652 -0.589861 -0.001240
N4 -0.131692 2.130525 -0.410501
N5 2.474603 -1.608735 -0.273891
N6 -1.776873 -0.352597 -0.382518
O7 -0.999828 0.055153 0.599680
O8 -2.639114 -1.121702 -0.013210

$NCNC(\text{-}ONO)N^-$
N1 0.974198 -0.529849 0.274408
C2 0.159376 0.519340 0.148487
C3 2.252837 -0.438529 -0.005575
N4 0.300109 1.726347 -0.236083
N5 3.402669 -0.485739 -0.220063
N6 -1.929508 -0.332689 -0.469797
O7 -1.184002 0.203790 0.587488
O8 -3.029191 -0.595211 -0.124579

TS8′
N1 -0.544933 0.025182 0.074622
C2 -0.934518 1.285770 -0.011630
C3 -1.357861 -0.997793 -0.125846
N4 -1.232220 2.409118 -0.075474
N5 -2.018796 -1.940951 -0.297633
N6 2.098371 -0.663667 0.106354
O7 2.455328 0.196169 -0.648520
O8 0.749336 -0.263124 0.919742

$ON(CN)_2^-$
N1 -0.000069 0.336501 0.000000
C2 -0.000012 -0.330654 -1.151607
C3 -0.000012 -0.330654 1.151607
N4 -0.000012 -0.873522 -2.183473
N5 -0.000012 -0.873522 2.183473
O6 0.000099 1.730206 0.000000

NO
N1 0.000000 0.000000 -0.612285
O2 0.000000 0.000000 0.535749

Cartesian coordinates for the structures in Fig. 7, calculated at B3LYP/6-311++G(d,p)

[$MAT^+ - H_{C5}^+$]

C1 0.015014 -1.000571 0.000013
N2 1.065040 -0.116546 0.000016
N3 -1.017538 -0.137805 -0.000014
C4 -2.427131 -0.491209 -0.000026
H5 -2.913334 -0.086433 -0.889292
H6 -2.913335 -0.086509 0.889274
C7 0.615903 1.181366 -0.000007
H8 1.265779 2.040865 -0.000011
H9 -2.494976 -1.576533 -0.000071
N10 -0.681469 1.208355 -0.000025
N11 2.434751 -0.439357 0.000037
H12 2.613828 -1.015683 0.817842
H13 2.613835 -1.015751 -0.817718

NO_2

N1 0.000000 0.000000 0.321839
O2 0.000000 1.099987 -0.140804
O3 0.000000 -1.099987 -0.140804

precursor 1

C1 -0.286450 0.123468 0.465227
N2 -0.742895 -1.131660 0.165112
N3 -1.329789 0.873173 0.079221
C4 -1.423336 2.322617 0.155730
H5 -2.244595 2.607775 0.815074
H6 -1.600796 2.734133 -0.838802
C7 -2.005233 -1.065685 -0.369915
H8 -2.567029 -1.929832 -0.683946
H9 -0.481323 2.695519 0.551091
N10 -2.405834 0.168161 -0.434400
N11 -0.053594 -2.345941 0.342051
H12 0.860243 -2.240969 -0.093623
H13 0.100059 -2.472921 1.338833
N14 2.284570 0.366051 -0.265309
O15 2.810730 1.370950 0.106883
O16 2.683814 -0.769025 -0.332084

precursor 2

C1 -0.279087 0.059472 0.463816
N2 -0.855949 -1.135681 0.120858
N3 -1.255344 0.912897 0.112249
C4 -1.215989 2.360718 0.238004
H5 -2.003041 2.697918 0.914640
H6 -1.361800 2.820944 -0.740355
C7 -2.108675 -0.935883 -0.403735
H8 -2.748241 -1.732386 -0.746572
H9 -0.240530 2.631784 0.634304
N10 -2.394598 0.330611 -0.420739
N11 -0.281491 -2.414039 0.244386
H12 0.634396 -2.372947 -0.195267
H13 -0.128967 -2.590049 1.233979
N14 2.948220 0.281311 0.004980
O15 2.615825 -0.853544 -0.191317
O16 2.427277 1.330195 -0.223856

TS9

C1 -0.061475 -0.143473 0.341342
N2 -0.175243 1.203211 0.062532
N3 -1.325747 -0.590125 0.158874
C4 -1.799360 -1.953991 0.305369
H5 -2.174925 -2.322382 -0.650518
H6 -2.597515 -1.990241 1.049055
C7 -1.480618 1.474752 -0.260295
H8 -1.829116 2.465041 -0.503133
H9 -0.962897 -2.569452 0.628894
N10 -2.212175 0.403655 -0.218948
N11 0.823198 2.182836 0.134734
H12 1.277269 2.095316 1.039959
H13 1.526443 1.970472 -0.569316
N14 2.264958 -1.100440 -0.344065
O15 2.641446 -0.315147 0.486551
O16 1.006619 -1.010658 -0.719719

TS10

C1 0.055851 -0.025598 0.526961
N2 0.497704 1.221212 0.154265
N3 1.058800 -0.828949 0.118398
C4 1.150980 -2.271539 0.284630
H5 1.934390 -2.513598 1.005693
H6 1.386813 -2.728806 -0.676290
C7 1.720356 1.094054 -0.452616
H8 2.278929 1.933388 -0.832762
H9 0.187189 -2.632519 0.635481
N10 2.098872 -0.148523 -0.487711
N11 -0.149109 2.451743 0.353183
H12 -1.094829 2.347436 -0.013319
H13 -0.219337 2.611229 1.355296
N14 -1.650382 -0.406356 -0.176891
O15 -2.019143 -1.558522 -0.095533
O16 -2.359291 0.580707 -0.324050

TS11

C1 -1.109628 -0.796083 0.527592
N2 -0.291432 0.332637 0.582802
N3 -2.171814 -0.277913 -0.094355
C4 -3.387219 -0.994678 -0.450088

H5 -3.529163 -0.964864 -1.531193
H6 -4.244937 -0.532192 0.040118
C7 -0.922595 1.419778 -0.014009
H8 -0.485531 2.401735 -0.105964
H9 -3.272122 -2.022339 -0.114834
N10 -2.091040 1.074974 -0.438599
N11 0.922016 0.319175 1.176128
H12 1.704897 -0.555632 0.755624
H13 1.345712 1.244563 1.093815
N14 3.220831 -0.473638 -0.655666
O15 2.563467 -1.221119 0.150206
O16 2.921267 0.699617 -0.714044

5-O-MAT
C1 0.015229 0.692754 0.000000
N2 1.094223 -0.207119 0.000001
N3 -1.063216 -0.158907 -0.000001
C4 -2.455049 0.236577 0.000001
H5 -2.958459 -0.144373 0.890923
H6 -2.958465 -0.144386 -0.890912
C7 0.594741 -1.484263 -0.000001
H8 1.223330 -2.360008 0.000000
H9 -2.483918 1.325658 -0.000006
N10 -0.700909 -1.492417 -0.000001
N11 2.446018 0.136378 -0.000001
H12 2.631817 0.709796 -0.819421
H13 2.631826 0.709777 0.819430
O14 0.068942 1.910948 -0.000001

5-O_2N-MAT
C1 0.050171 0.117743 0.032569
N2 0.647462 -1.128695 -0.009119
N3 -1.288623 -0.129182 0.039107
C4 -2.415632 0.794844 -0.056905
H5 -3.229485 0.377969 0.534625
H6 -2.730092 0.889030 -1.098949
C7 -0.365028 -2.044111 -0.053419
H8 -0.182311 -3.105181 -0.095690
H9 -2.100025 1.761665 0.321916
N10 -1.534790 -1.480826 -0.024324
N11 2.008754 -1.468266 0.070228
H12 2.502769 -0.682673 -0.360449
H13 2.270654 -1.459749 1.055829
N14 0.707264 1.314171 -0.003316
O15 0.044283 2.375052 0.202886
O16 1.964587 1.282157 -0.252734

[$MAT^+ - H_2^+$]
C1 -0.037674 -1.023878 0.000001
N2 -1.137895 -0.160312 0.000001
N3 0.958833 -0.134759 -0.000001
C4 2.380602 -0.439288 -0.000003
H5 2.849516 -0.015975 0.889531
H6 2.849514 -0.015973 -0.889536
C7 -0.707238 1.159406 0.000000
H8 -1.378853 2.002093 0.000001
H9 2.486312 -1.521398 -0.000004
N10 0.583316 1.213191 -0.000001
N11 -2.433283 -0.503345 0.000003
H12 -2.417419 -1.529613 0.000004

***cis*-HNO_2**
N1 0.172216 -0.519525 -0.000064
O2 1.058432 0.258769 0.000007
O3 -1.090084 0.066242 0.000032
H4 -0.952299 1.036586 0.000138